

Apicella, M., et al. *Some recent results at ENEA. in The 12th International Conference on Condensed Matter Nuclear Science. 2005. Yokohama, Japan.*

SOME RECENT RESULTS AT ENEA

M. APICELLA, E. CASTAGNA, L. CAPOBIANCO, L. D'AULERIO, G. MAZZITELLI,
F. SARTO, A. ROSADA, E. SANTORO, AND V. VIOLANTE
ENEA Frascati Research Center V.le E. Fermi, 45 00044 Frascati (RM), Italy

M. MCKUBRE AND F. TANZELLA
SRI International, 333 Ravenswood Ave., Menlo Park, CA 94025, USA

C. SIBILIA
La Sapienza University, Via Scarpa, 14 00100 (Roma), Italy

Recent research activity at ENEA, in the field of Condensed Matter Nuclear Science, has been oriented to material science and Laser triggering in order to increase the reproducibility of excess of power production during loading of palladium with deuterium. Isoperibolic calorimetry in gas phase, isoperibolic and flow calorimetry with electrochemical systems have been carried out. Nuclear ashes detection was done by means of high resolution and high sensitivity mass spectrometer. Material science studies allowed to obtain a palladium showing high solubility for hydrogen isotopes and giving deuterium concentration at equilibrium larger than 0.95 (as D/Pd atomic fraction) with a reproducibility larger than 90%. Excess of power production by using the above-mentioned material achieves a reproducibility up to 30% without triggering. Laser irradiation with a proper polarization seems to have a significant role in further increasing of the excess of power production reproducibility. Heat bursts exhibit an integrated energy at least 10 times greater than the sum of all possible chemical reactions within a closed cell. The energy gain calculated at the end of the experiments is observed with deuterium but not with hydrogen. Preliminary measurements give a ${}^4\text{He}$ signal in reasonable agreement with the expected values by assuming a $\text{D} + \text{D} = {}^4\text{He} + \text{heat}$ (24 MeV for event) reaction.

1. Introduction

The dissolution of hydrogen isotopes into a metal lattice is not only a problem of thermodynamic equilibrium between the hydrogen inside the lattice and the hydrogen in the external phase (gas or liquid) but is also a problem of not equilibrium because of the occurrence of a transport process. Both aspects of the phenomenon are correlated since the equilibrium concentration of the solute is achieved when the chemical potentials of the hydrogen in both phases are equal and since the transport process inside the metal lattice is driven by the gradient of the chemical potential.

The migration of interstitials in a metal under an applied external bending is well known as Gorsky effect.¹ The deformation field produces the defects migration

toward the expanded areas. Lewis and co-workers²⁻⁴ showed that internal stresses are generated during insertion and diffusion of interstitial hydrogen and that the resulting strain production represents an opposing force to the flux produced by the concentration gradient.

The effect of the stress as limiting factor in achieving the deuterium-loading threshold in palladium to have excess of power production is studied.

2. Stress Field Limiting Hydrogen (Deuterium) Solubility in Palladium

The chemical potential of the hydrogen in solid solution in a metal lattice is strongly influenced by all field force, like the stress field, modifying the free energy of the system. The hydrogen isotopes dissolving into a metal (i.e. palladium) occupies interstitial positions and expands the lattice. This process generates a stress field when remarkable concentration differences (strong gradients or coexistence of different phases) are created. The situation is quite similar to the stress produced by a temperature gradient as shown in Fig. 1.

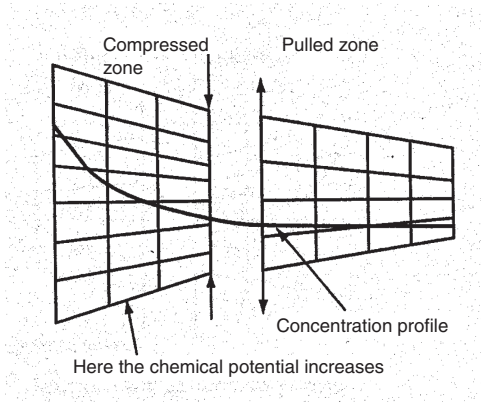


Figure 1. The effect of the hydrogen concentration profile on the stress field.

Therefore, the loading process may be inhibited by a stress gradient, for instance behind the external surface, where the effect is traceable to the effect of a strong temperature gradient. Thus, in the zone at high concentration, compressed by the zone at low concentration, the chemical potential of the solute increases and the loading can be inhibited.

In the following such a problem will be approached in order to have an analytical tool to estimate the effect of the stress field on the loading and to identify the metallurgical conditions that can reduce this effect allowing the increasing of the amount of hydrogen dissolved in the metal. Chemical potential of hydrogen

dissolving into a metal lattice, in presence of a stress field, becomes⁵

$$\mu_s = \mu_s^* - \frac{\bar{V}_s}{3} (\sigma_{xx} + \sigma_{yy} + \sigma_{zz}) = \mu_s^* - \bar{V}_s \text{tr } \bar{\sigma} \equiv \mu_s^* - \bar{V}_s \sigma_h, \quad (1)$$

where μ_s^* is the hydrogen chemical potential into the lattice without stress, \bar{V}_s is the partial molar volume of the solute and σ_h the trace of the stress tensor.

3. Flux Equation with a Stress Field

A diffusive flux of hydrogen within a homogeneous and solid media is created by a gradient of chemical potential and by the field of the applied forces so that the expression for the flux is

$$\bar{J} = -Mc \frac{\partial \mu}{\partial c} \frac{\partial c}{\partial x} + Mc \bar{F}, \quad (2)$$

where M is the mobility, c the solute concentration, and \bar{F} is the vector given by the sum of the applied forces acting on the hydrogen interstitially dissolved in the solid.

By replacing the relationship between diffusion coefficient and chemical potential, $D = Mc(\partial \mu / \partial c)$, into Eq. (2) it follows:

$$\bar{J} = -D \nabla c + \frac{D \bar{F} c}{c(\partial \mu / \partial c)}. \quad (3)$$

A little of algebra leads to

$$\bar{J} = -D \nabla c + D \frac{\bar{F}}{RT} c. \quad (4)$$

For a stress field the flux equation becomes:

$$J = -D \left(\nabla C - \frac{C \bar{V}}{RT} \nabla \sigma \right), \quad (5)$$

where σ is the local stress. The analysis allows us to study the mass transfer problem when the stress field is created during the loading. In the following, we will consider a system where the diffusion is well described by one-dimensional time-dependent model (foil, membrane or wire).⁶

By introducing the fraction of relaxed stress η into the flux equation it follows:

$$J^d = D \left(-\frac{\partial c}{\partial x} + (1 - \eta) \frac{\bar{V}}{RT} c \frac{\partial \sigma}{\partial x} \right). \quad (6)$$

A mass balance on a foil leads to:

$$\frac{\partial c}{\partial t} = D \frac{\partial}{\partial x} \left(\frac{\partial c}{\partial x} - (1 - \eta) \frac{\bar{V}}{RT} c \frac{\partial \sigma}{\partial x} \right). \quad (7)$$

Let us to consider the well-known stress (σ) strain (ε) relationship:

$$\sigma = E\varepsilon, \quad (8)$$

where E is the Young's module. The relationship between strain and concentration for Pd β -phase (assuming that it may be extrapolated up to a loading atomic fraction close to one)

$$\varepsilon(\bar{c}) = [1 + b(\bar{c} - \bar{c}_{\beta \min})], \quad (9)$$

where $\bar{c}_{\beta \min}$ is the hydrogen concentration value for the $\alpha + \beta$ phases coexistence limit, $b = 0.044$ and $\bar{c} = c/c_0$ the dimensionless concentration (c_0 is the metal atoms concentration). Let us introduce the following dimensionless parameters

$$\bar{x} = x/L, \quad \tau = L^2/D, \quad (10)$$

where L is the characteristic length of the system (typically the thickness or the radius), so that the resulting dimensionless transport equation is

$$\frac{\partial \bar{c}}{\partial \tau} = \frac{\partial^2 \bar{c}}{\partial \bar{x}^2} - (1 - \eta)b \frac{\bar{V}E}{RT} \left(\frac{\partial \bar{c}}{\partial \bar{x}} \right)^2 - (1 - \eta)b \frac{\bar{V}E}{RT} \bar{c} \frac{\partial^2 \bar{c}}{\partial \bar{x}^2}, \quad (11)$$

where we introduced η as a parameter giving the percentage of stress that is released by plastic deformation or by dislocation slipping; it is clear that when the release of the stress is complete the transport equation reduces to the Fick's one.

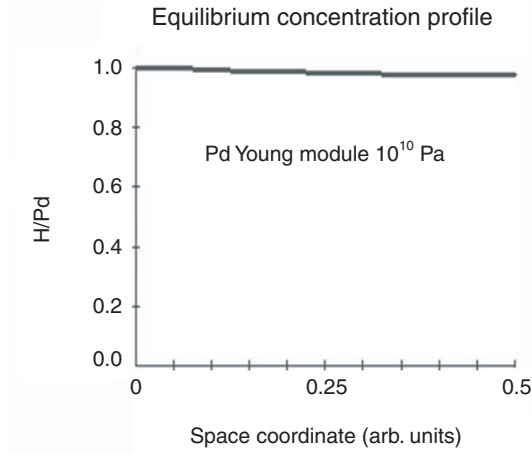


Figure 2. Equilibrium H concentration profile within a Pd foil with Young's module = 10^{10} Pa.

Equation (11) describes the interstitial diffusion of hydrogen into a metal (e.g. palladium) under a stress field. The effect of stress at steady state translates on a different concentration profile, then a different loading that depends on the properties of the material such as the Young's module.

The transport equation (11) is solved with the boundary conditions $\bar{c} = 1$, $\bar{x} = 0$ and $\partial \bar{c} / \partial \bar{x} = 0$, $\bar{x} = L/2$ and including the calculation of the relaxed stress on the basis of the mechanical properties of the material (σ_r). Some calculations have been done by using indicative values of the Young's module in order to make more

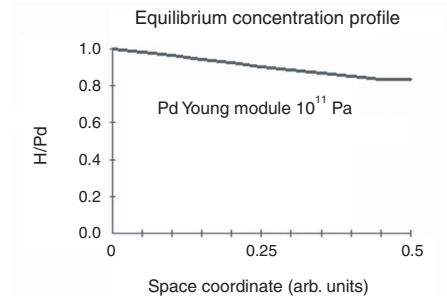


Figure 3. Equilibrium H concentration profile within a Pd foil with Young's module = 10^{11} Pa.

clearer the effect. Figures 2 and 3 show the equilibrium concentration profile, from the external side up to the symmetry plane, for two palladium foils with different Young's module. In the first case the value of the Young's module is 1.0×10^{10} Pa while in the second case the value is 1.0×10^{11} Pa (these value are chosen in order to magnify the effect). It is clear that the loading reduces when the Young's module increases. The calculation of the concentration profiles evolutions has been used to calculate also the evolution of the R/R_0 ratio by assuming the foil as a parallel of electric resistances and by considering the well-known Baranowsky curves. Figures 4 and 5 show the evolution of the R/R_0 ratio for the two considered above-described loading conditions.

Figures 4 and 5 reproduce typical situations that one may observe experimentally.

- (1) High loading: after achieving the maximum the R/R_0 reduces to 1.4 and to 1.6 for H and D, respectively.
- (2) Low loading: after achieving the maximum R/R_0 reduces only a little bit since the dissolution of H or D stops because of the stress (unless a contaminant on the surface inhibits the dissolution of H or D).

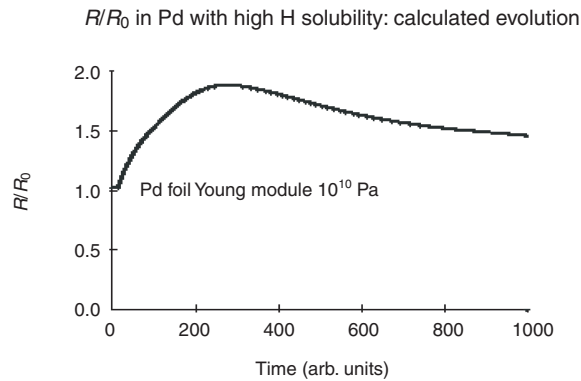


Figure 4. Calculated evolution of R/R_0 for high solubility (reduced stress) material.

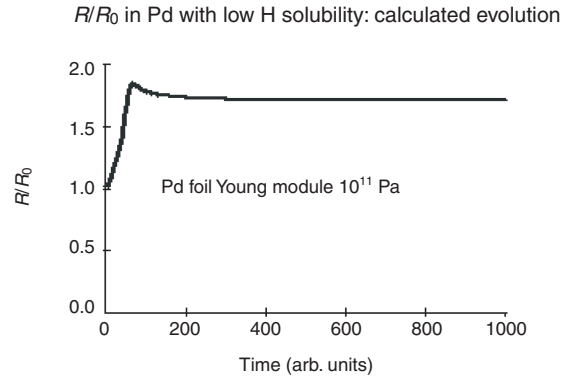


Figure 5. Calculated evolution of R/R_0 for low solubility (high stress) material.

The model allowed us to seek for a material showing a homogeneous loading able to minimize the concentration gradients and then the stress field. Some treatments, based on cold and annealing steps allowed us to optimize metallurgical structure of the materials in order to increase the H(D) loading. The row material was palladium foil 0.5 mm thick able to reach a loading ratio of about 0.8 (hydrogen atomic ratio). The treatment has been done in two steps:

1. Cold rolling of the row material leading Pd foil 50 μm thick.
2. Annealing at different temperatures (ranging from 700 and 1100°C) for different times.

Figure 6 shows a simply cold worked sample. Figure 7 shows the effect of the annealing (1100°C for 5 h) after rolling, the sample microstructure is changed and it is clear the growth of the grains. Figure 8 shows the microstructure of a sample annealed for 1 h at 850°C after rolling.

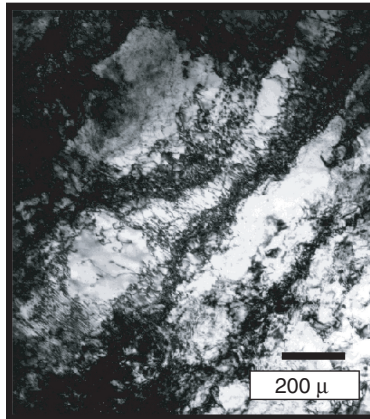


Figure 6. Cold worked palladium.



Figure 7. Palladium annealed at 1100°C for 5 h.

Figure 9 shows the effect of the treatment (i.e. of the metallurgical structure on the H (D) loading). $H/Pd = 0.97$ has been obtained in the sample cold worked and annealed at 850°C for 1 h.

A possible interpretation of such a results is that in the last considered sample the concentration profiles are maintained relatively flat because of the reduced size of the grains. The above-described tests have shown a satisfactory reproducibility.

Another interesting effect found in the experiments is the correlation, that some time occurs, between the loading dynamics and the loading ratio. One may observe that after loading at constant current density for a certain time, the concentration of the solute in the metal does not increase any more and sometimes a de-loading takes place. On the basis of the concepts exposed in the previous section, we assumed that such a behavior was promoted by the creation of a stress field very close to the surface of the sample under the electrochemical loading. Stress removal has been performed by applying a low-high current mode, just to avoid the creation of a new stress field. The effect of this technique is well described in Ref. 6.



Figure 8. Pd cold worked and annealed at 850°C for 1 h.

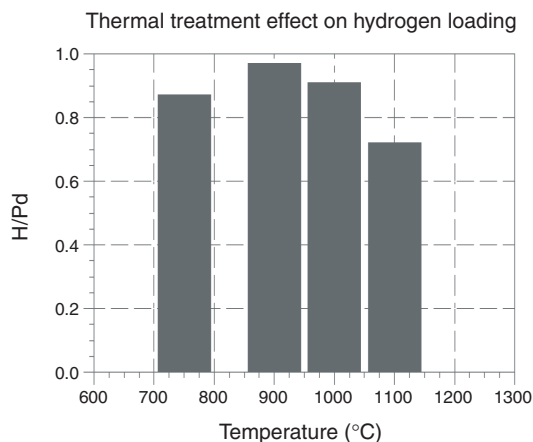


Figure 9. Effect of the thermal treatment on the loading.

4. Calorimetric Results

Flow and isoperibolic calorimetric measurements have been performed by using pre-treated palladium into electrochemical cells with LiOD 0.1 M electrolyte.

4.1. Flow Calorimetry

Excess of power measurements has been carried out by using a flow calorimetric system composed by a Memmert thermostatic box ($\pm 0.05^\circ\text{C}$), Haake thermostatic bath for coolant water, Bronkhorst high precision mass flow meter and controller ($0.3\text{--}0.1\text{ cm}^3/\text{s}$), read by the data acquisition system in order to have a precise measurement of the output power. He leakage tested cell ($2 \times 10^{-10}\text{ mbar l/s}$) is immersed into a water jacket cooled by a water coolant pipe. Inlet and outlet

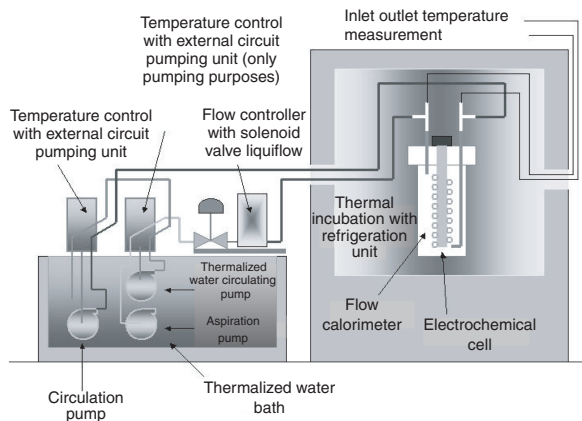


Figure 10. Flow calorimeter system.

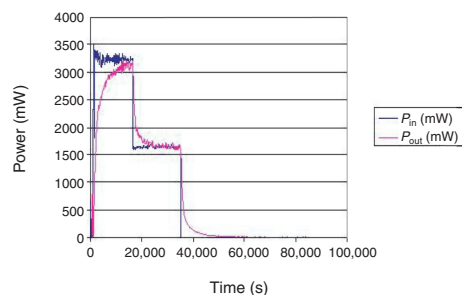


Figure 11. Input and output power during an experiment performed with LiOH 0.1 M electrolyte LiOH.

temperatures of the coolant are measured with two Pt 100 thermometers (four wires measurement). The closed electrochemical cell is equipped with a recombiner. Cell power supply is an AMEL galvanostat, modulated, during the HI-LO current mode by an HP 33120 wave function generator. Output power is measured by means of the mass flow rate and coolant temperatures, R/R_0 measurement is done by means of an HP-4284 (four wires measurement). Figure 10 shows a schematic view of the flow calorimetric system.

Several experiments have been done by using light water (LiOH 0.1 M electrolyte) obtaining a calorimeter efficiency of 97.5% (output = 0.975 input, because of the heat losses). No excess of power production has been observed by using H_2O despite a very high loading ($H/Pd = 0.97$) was always achieved.

A different behavior has been observed in several cases by using LiOD electrolyte. Excess of power has been obtained in C1, C3, and C4 experiments under high

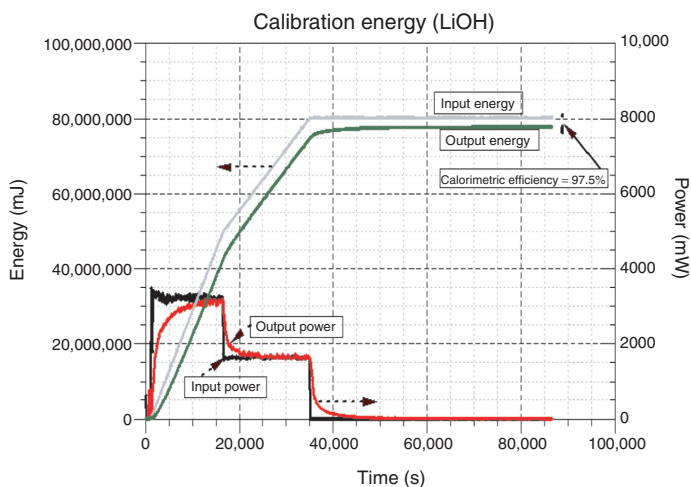


Figure 12. Plot of energy and power (input and output) for calibration with H_2O 0.1 M.

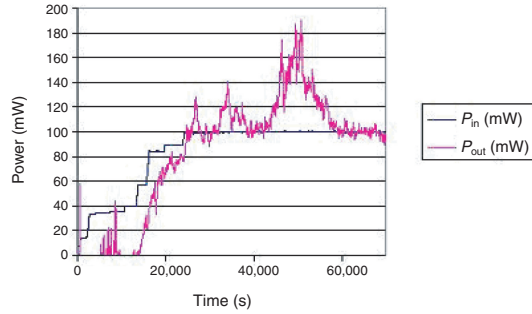


Figure 13. Experiment C3: excess of power versus time (input and output). C3 experiment: plot of energy and power.

loading of D into Pd ($D/Pd > 0.92$). Figures 11 and 12 show the input and output power and energy for an experiment that may be considered as a reference experiment performed with light water. No evidences of excess of power are observed and the output energy perfectly respects the efficiency of the calorimetric system that recover 97.5 of the input power, so that the output energy curves always maintains below the input.

Figures 13 and 14 show the C3 experiment evolution of the input and output power and energy. After 25,000 s, at high loading ($D/Pd > 0.92$) the output power overcame the input one and the bursts survived up to 60,000 s giving an output power 80% larger than the input.

Despite the short lifetime of the burst a completely different behavior, of the energy curves (Fig. 14) (if compared with the reference experiment) may be observed: during the excess of power production also the output energy curve overcome the input one. A similar behavior has been observed in C1 and C4 experiments. Three excesses of powers have been observed over nine experiments although the achieved D concentration in Pd (atomic fraction) was always larger than 0.9. Then the load-

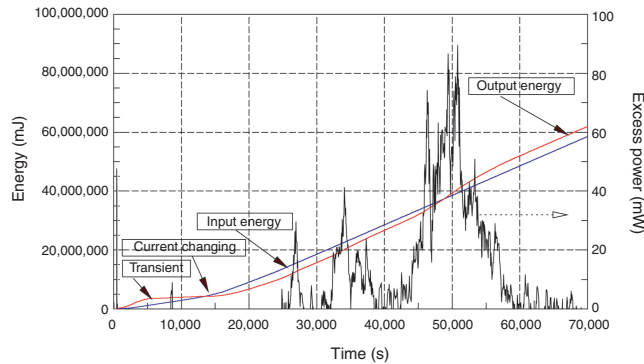


Figure 14. Isoperibolic calorimeter and electrochemical cell for Laser triggering.

ing threshold $D/Pd > 0.9$ is clearly only a *necessary condition*. An upgrade of the experiment has been conceived in order to increase the reproducibility of the excess of power production.

4.2. Isoperibolic Calorimetry under Plasmons–Polaritons Laser Triggering

An isoperibolic calorimetric system has been developed allowing a Laser irradiation during the electrochemical loading. According to the idea that collective electron oscillations have a key role in LENR processes a proper trigger has been introduced to create surface plasmons (polaritons).

Surface plasmons are quantum of plasma oscillations created by the collective oscillation of electrons on a solid surface. Surface plasmons may be generated by mechanisms able to produce *charge separation* between Fermi level electrons and a background of positive charges (i.e. lattice atoms):

1. Electrons beam.
2. Laser stimulation.
3. Lattice vibrations.
4. Charged particles interacting with a surface.

Laser triggering was selected because of its results to be the most appropriate under electrochemical loading. Needs to underline that plasmons are longitudinal plasma oscillations that do not couple with external radiation. A prism or cylindrical lens in contact with the surface to be irradiated with a Laser can be used in order to have the required coupling. The alternative is to irradiate a rough surface and for such a reason a proper acid etching has been done on the Pd samples used as cathodes into the electrochemical cell. In addition to that one may consider that a *p*-polarized Laser beam is the appropriate one to create charge separation on the surface of the specimen.

The electrochemical cell, equipped with two small glass windows was placed into a thermostatic box ($\pm 0.15^\circ\text{C}$) also equipped with a window for the Laser beam (5 or 33 mW, 632 nm) as shown in Figure 14. All the instrumentations and the data acquisition system are quite similar to the equipment above described for flow calorimetric system.

Four experiments have been carried out into the isoperibolic calorimetric system and have been labeled Lasers 1, 2, 3, 4. Laser 1 was a calibration done by using light water (0.1 M LiOH) and the calibration curve is shown in Fig. 15. Despite the behavior of the system was quite linear a proper fitting curve has been used in order to have $R^2 = 1$.

Laser 2 experiment was performed by using 0.1 M LiOD electrolyte in heavy water. After 320 h about a square wave current was applied in order to increase the D loading into the cathode, according to the effect described in Section 1 of the work. After achieving a loading D/Pd of about 0.94 a 632 red Laser of 5 mW was continuously applied under continuous current electrochemical conditions. An

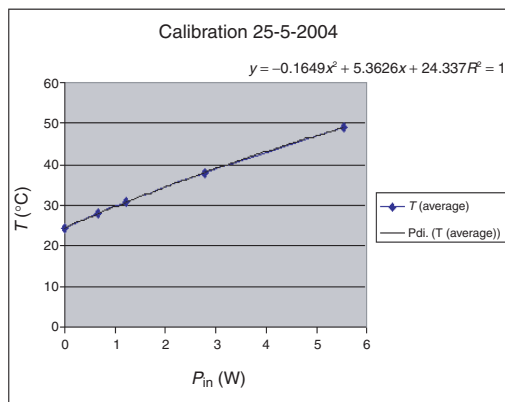


Figure 15. Calibration curve for isoperibolic calorimeter.

excess of power, ranging from 60 mW up to ≈ 300 mW (see Fig. 16), was revealed. At the end of the experiment the excess of energy was 23.5 kJ (17.3 MJ/mol Pd).

In Laser 3 experiment a 33 mW, 632 nm Laser was applied after achieving a loading $D/Pd = 0.95$ under square wave current mode. During the experiment the Laser polarization was changed from “*p*” to “*s*” and vice versa. The effect is shown in Figs. 17 and 18. Seems clear, as expected, that the excess of power takes place under “*p*” polarization and disappears by applying “*s*” polarization. An amount of 3.4 kJ of energy (2.5 MJ/mol Pd) was produced during the experiment.

Laser 4 experiment was carried out by applying a continuous electrochemical current. After achieving a loading threshold of 0.95 the cathode was continuously irradiated by using a 632 nm, 33 mW red Laser. Calorimetry gave 30.3 kJ of produced energy (19.4 MJ/mol Pd). Figure 19 shows the input and output power and energy evolution after applying the Laser irradiation.

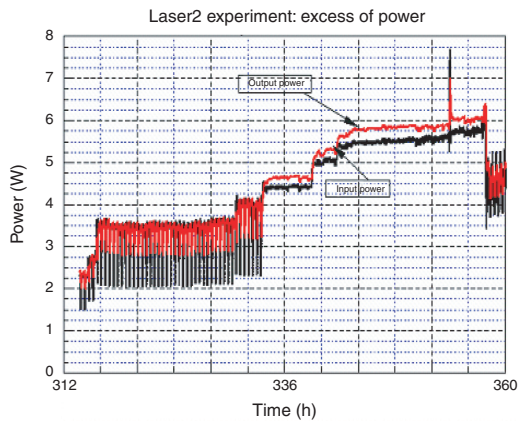


Figure 16. Evolution of the input and output power, last 30 h under Laser irradiation (*p*-polarization), 632 nm, 5 mW. ${}^4\text{He}$ production estimate 6.12×10^{15} .

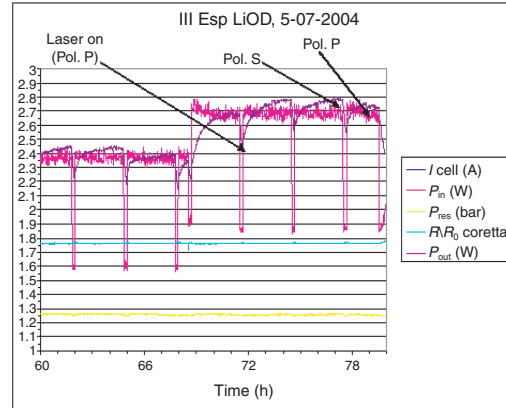


Figure 17. Excess of power under Laser triggering (p and s -polarization effect). 632 nm, 33 mW HI-LO current mode.

5. ^4He Measurements

Increasing of ^4He concentration in the electrochemical cell was expected, by assuming that the excess of energy produced was created by a $\text{D} + \text{D} = ^4\text{He} + 24 \text{ MeV}$ reaction. He tight cells (2×10^{-10} mbar l/s He leakage test) have been used in both flow and isoperibolic calorimeters. The gas in the cell was analyzed at the beginning of the experiment, during the experiment when no excess of heat was observed and at the end of the experiment. A gas sample was sent from the cell to an inlet system for the mass spectrometer.

All the manifolds were realized by using VCR fitting and maintained under baking before and during measurements. The manifold is under vacuum at 2×10^{-5} mbar before sending a gas sample. The whole line was checked for He

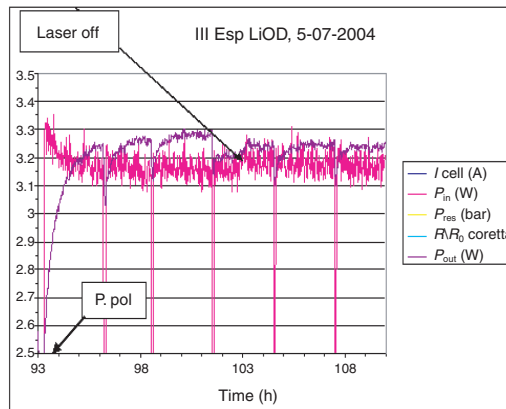


Figure 18. Excess of power under Laser triggering (Laser off effect). HI-LO current mode.

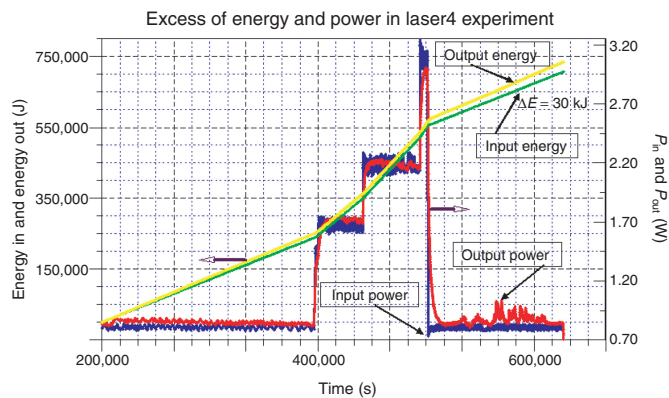


Figure 19. Excess of energy and excess of power in Laser 4 experiment.

leakage giving 10^{-10} mbar l/s. A 707 Saes getter was used to trap deuterium, oxygen and nitrogen from the sample gas before sending it to the MS.

Figure 20 shows a scheme of the system. The mass spectrometer used was a high resolution and high sensitivity Jeol CG-Mate. Figure 21 shows the resolution for mass 4. It is clear that the resolution is high enough to separate ^4He and D_2 (resolution limit is 10^{-4} amu).

Figure 22 shows the results of the analysis giving the ^4He concentration measured in the cells at the end Lasers 2–4, experimental values are also compared with the expected values and with the background.

6. Conclusions

Heat effects are observed with D, but not with H, under similar (or more severe) conditions.

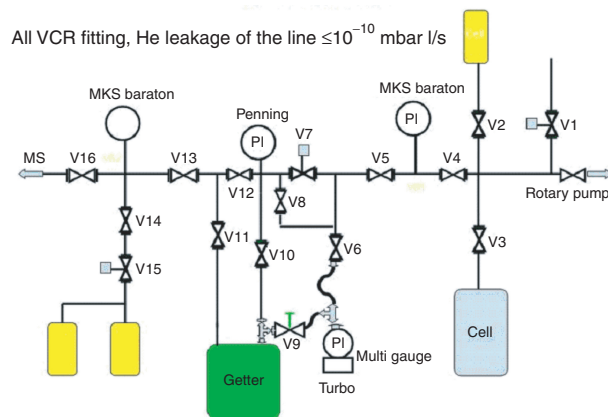


Figure 20. Mass spectrometer inlet line.

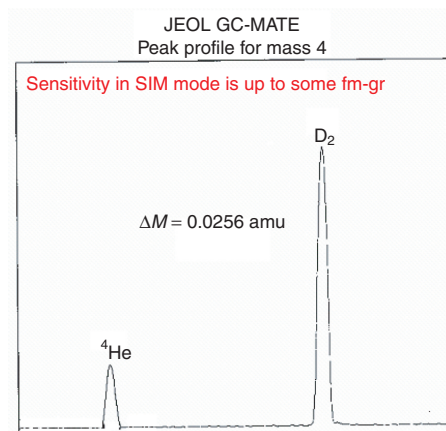


Figure 21. Jeol GC Mate mass 4 resolution.

Heat bursts exhibit an integrated energy at least $10 \times$ greater than the sum of all possible chemical reactions within a closed cell. Experiments reproducibility was significantly improved as a result of material science study. Some conditions are required to have a reproducible excess of power:

1. Loading threshold $\text{D}/\text{Pd} > 0.9$ (*necessary condition*).
2. Suitable material to have a reproducible loading above the threshold.
3. Trigger.
4. Suitable status of the material to have coupling with trigger.

Three excess of power over three effective experiments have been achieved by respecting these conditions during electrochemical experiment! The accordance

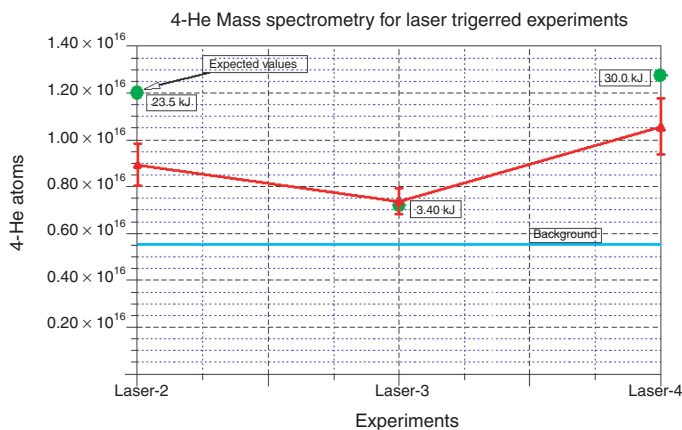


Figure 22. The expected amount of increasing of ^4He is in accordance with the energy gain by assuming a $\text{D} + \text{D} = ^4\text{He} + 24 \text{ MeV}$ reaction.

between revealed ^4He and produced energy seems to be a clear signature of a nuclear process occurring in condensed matter.

Acknowledgments

The authors would like to thank Dr. Guido Petrini of Sued Chemie for his support for all the scientific aspects concerning catalytic materials. In particular, for giving both the catalysts that have been used for MATRIX experiment and for closed electrochemical cells. Dr. R. Hartens, Dr. O. Seguin, Dr. S. Quill, Dr. A. Kusai, and Dr. F. Dalia of JEOL for their help in optimizing for the experiments the JEOL JC-Mate Mass spectrometer used. Mr. D. Lecci, Mr. F. Marini, Mr. Polinari, Mr. Marcelli, and Mr. Bettinali of ENEA for their technical support. Dr. S. Lesin, Dr. A. El Boher, and Dr. Tanya Zilov of Energetics Technologies Ltd. for the very useful interaction that positively affected the research work.

References

1. H. Wipf, *J. Less-Common Met.* **49**, 291 (1976).
2. F. A. Lewis, J. P. Magennis, S. G. McKee, and P. J. M. Sebuwufu, *Nature* (London) **306**, 673 (1983).
3. F. A. Lewis, B. Baranowski, and K. Kandasamy, *J. Less Common Met.* **134**, L27 (1987).
4. F. A. Lewis, X. Tong, K. Kandasamy, R. V. Bucur, and Y. Sakamoto, *Electrochem. Acta* **218**, 57 (1993).
5. R. A. Oriani, *Trans. Fusion Technol.* **26**, 235–266 (1994).
6. A. De Ninno, A. La Barbera, and V. Violante, Consequences of lattice expansive strain gradients on hydrogen loading in palladium. *Phys. Rev. B*, **56** (5), 2417–2420 (1997).